Journal of Medicinal Chemistry

Article

pubs.acs.org/jmc

Quantitative and Site-Directed Chemical Modification of Hypocrellins toward Direct Drug Delivery and Effective Photodynamic Activity

Hong Deng,[†] Xin Liu,[†] Jie Xie,*[,†] Rong Yin,[‡] Naiyan Huang,[‡] Ying Gu,*[,‡] and Jingquan Zhao*[,†]

[†]Beijing National Laboratory for Molecular Sciences (BNLMS), Key Laboratory of Photochemistry, Institute of Chemistry, Chinese Academy of Sciences, Beijing 100080, People's Republic of China

[‡]Department of Laser Medicine, Chinese PLA General Hospital, Beijing 100853, People's Republic of China

Supporting Information

ABSTRACT: For photodynamic therapy (PDT) treatment of microvascular diseases, drugs are delivered via blood circulation and the targets are vasculature endothelial cells, for which the contradictory requirements of hydrophilicity and lipophilicity of the drugs have been achieved by liposome preparations. Herein, it is demonstrated that the drug delivery and target affinity are achieved by a single chemical compound, hypocrellin B (HB) derivative **6** selected from three novel aminoalkanesulfonic acid HB derivatives, **5**–**7**. **6** exhibits a much higher PDT activity (IC_{50} = 22 nM) on human gastric carcinoma BGC823 cells than HB, while it has no cellular toxicity in the dark. On the basis of estimation of the clinically required concentration according to relative PDT activity and clinical criteria, it can be predicted that **6** is directly deliverable to and PDT effective on target cells. The enhanced red absorption and superhigh photoactivity suggest that **6** is more powerful for PDT of tumors than HB.

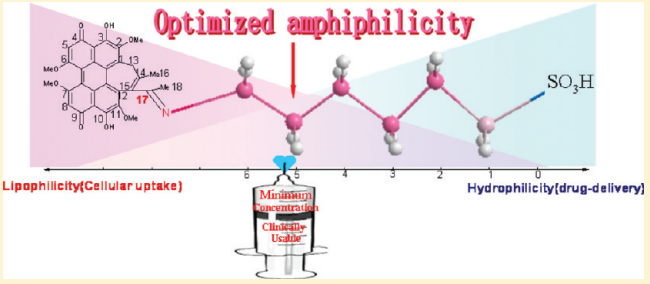

INTRODUCTION

In recent years, photodynamic therapy (PDT) has become a powerful clinical treatment of various diseases.[1,2] In principle, PDT depends on selective destruction of the targets by singlet oxygen or other reactive oxygen species (ROS) generated jointly by photosensitizers (drugs), light (usually a laser), and oxygen. Compared to well-developed lasers, clinically usable photosensitizers (drugs) specifically aimed at individual disease are seriously deficient.[3] An ideal PDT drug should satisfy some criteria, including strong absorption during the "photo-therapeutic window", high photoactivity but low dark toxicity, high affinity for target cells but fast clearance from tissues, and ready deliverability in vivo.[4] Hypocrellins, including hypocrellin A (**1**) and hypocrellin B (**2**) (shown in Chart 1), photo-sensitizers isolated originally from wild *Hypocrella bambusae* but recently synthesized chemically or biologically,[5,6] exhibit most of these advantages;[7−10] however, low absorption during the phototherapeutic window (600−900 nm) is a serious drawback for PDT of solid tumors,[11,12] while strong lipophilicity restricts drug delivery. Compared to solid tumors, some microvascular diseases, such as age-related macular degeneration (AMD) and port wine stains (PWSs), commonly occur on shallow surfaces (no more than 1 mm), which just coincides with the tissue-penetration depth of light from 500 to 600 nm.[13,14] Therefore, hypocrellins may be characteristic photosensitizers specifically suitable for PDT of microvascular diseases. Aqueous solubility is essential for bioavailability of a drug,[15] and even more important for those specifically aimed at microvascular diseases because the drug is delivered via intravenous injection.

Chart 1. Structures of 1−7

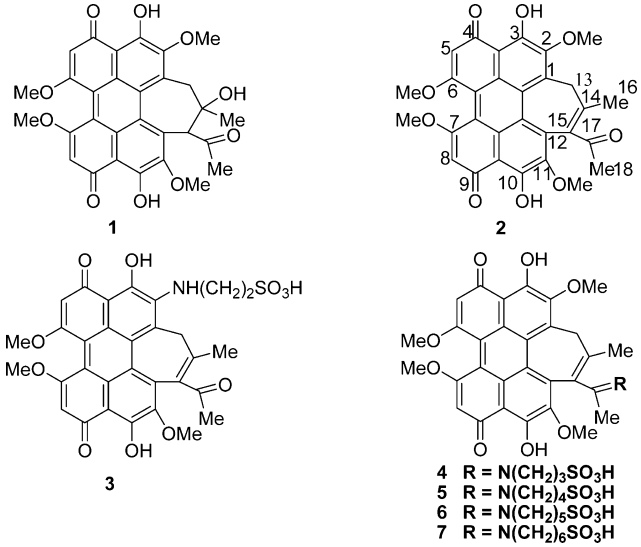

Lipophilic **1** and **2** are favorable for cellular uptake, but they may aggregate in blood and therefore block vascular nets. On the other hand, water-soluble derivatives are readily deliverable but commonly exhibit low PDT activity due to poor cellular uptake.[12] To satisfy the contradictory requirements of hydro-

Received: June 23, 2011
Published: February 21, 2012

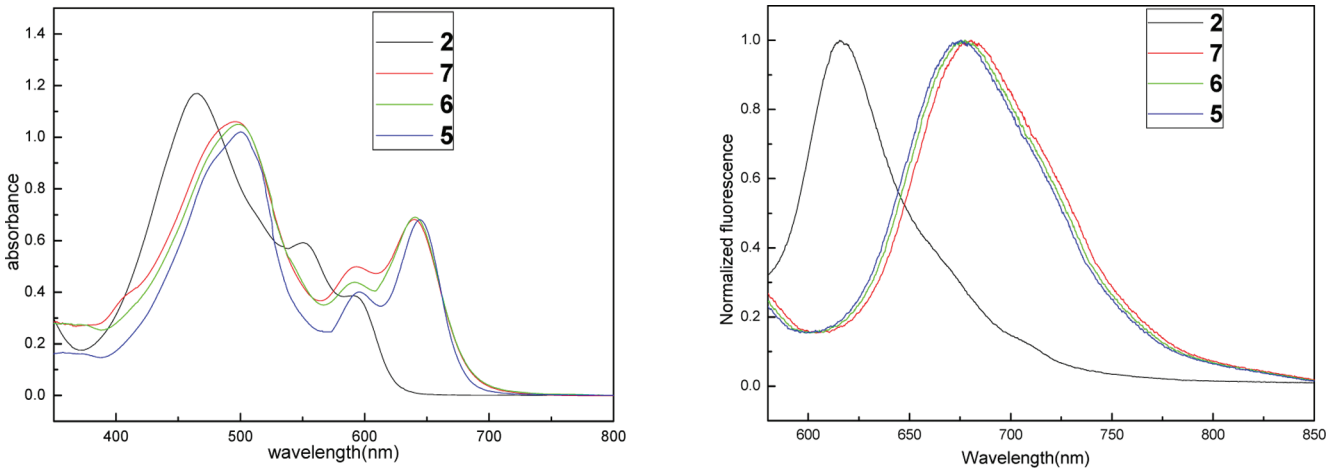

Figure 1. Absorption (left) and fluorescence emission (right, excited at 470 nm and normalized to the maximum) spectra of compounds **2** and **5**–**7** at the same concentration of 50 μM in dimethyl sulfoxide.

philicity and lipophilicity, a pharmaceutical strategy is to use drug-delivery vehicles such as liposomes or water-soluble particles.[16−18] However, a large amount of low-density lipoproteins or other photoinactive materials may burden blood circulation and reduce the effective drug concentration. Alternatively, a chemical strategy is to find a compromise between the lipophilicity and hydrophilicity—amphiphilicity. In the past two decades, about 50 hypocrellin derivatives were synthesized by introducing polar groups, and most of them were announced to be "amphiphilic", but the amphiphilicity had only relative significance. Furthermore, it was found that any improvement in the aqueous solubility would unexceptionally lead to the PDT activity being sacrificed.[12,19] From a medicinal chemistry view, amphiphilicity or aqueous solubility should be quantitative rather than qualitative, which can be defined as the aqueous solubility being equal to or larger than the clinically required concentration while the lipophilicity remains as high as possible. Noticeably, sulfonated hypocrellin is completely water soluble,[20] but loses biological PDT activity, while taurine- or aminopropanesulfonic acid-substituted hypocrellin B (**3** and **4**, Chart 1) shows a sequential decrease in aqueous solubility but an increase in PDT activity,[21,22] implying that the aqueous solubility may be quantitatively regulated by a step lengthening the alkyl chain in the substitutent.

Besides cellular uptake, photosensitization activity, mainly evaluated by the singlet oxygen yield, is another key important factor for the PDT effect. It was reported that the PDT activity of pegylated distyrylboron dipyrromethene derivatives depend greatly on the types of substituents,[23] which may be a complex result of cellular uptake and photosensitizing activity. Besides what has been mentioned, another advantage of hypocrellins is that the chemical structures are readily modifiable by introducing various substituent(s) to site 2, 5, 8, 11, 13, 14, or 17, but singlet oxygen yields of the derivatives vary greatly. Generally, 2-, 5-, or 8-substituted derivatives exhibit a low singlet oxygen ($^1O_2$) yield[24−27] and 13-, 14-, or 17-substituted derivatives a higher $^1O_2$ yield.[22,28,29] Especially the singlet oxygen yield for 17-(3-amino-1-propanesulfonic acid)-substituted hypocrellin B Schiff base (**4**) is almost comparable to that of the parent **2**;[22] however, it was synthesized in strong alkali solution in a yield of no more than 10%.

In the current work, 17-(4-amino-1-butanesulfonic acid)-, 17-(5-amino-1-pentanesulfonic acid)-, and 17-(6-amino-1- hexanesulfonic acid)-substituted hypocrellin B (**5**–**7**, Chart 1), novel aminoalkanesulfonic acid-substituted hypocrellin B derivatives with a step increase in the carbon atom number of the alkyl chain, were synthesized in much higher yield (30%). Remarkably, the three derivatives exhibit much higher singlet oxygen yields (0.94 ± 0.01, 0.98 ± 0.01, 1.01 ± 0.01) than **2** (0.76). In vitro biological experiments confirmed that the PDT activity of **6** was far higher than those of **5** and **2**. On the basis of the relative PDT activity, aqueous solubility, and clinically required concentration, it was estimated that just **6** achieved the optimized amphiphilicity and could be directly deliverable via intravenous injection without the need for any drug-delivery vehicle.

RESULTS AND DISCUSSION

pH-Dependent Yield. Up to now, 17-substituted Schiff base derivatives of hypocrellins were all synthesized in strong alkali solution (pH > 12), which was necessary to prevent the amino group, with an isoelectric point at around 9.0,[30] from protonating, but the yields were very low (no more than 10%).[22,31] In fact, at pH > 12, **2** presents mainly in the form of a double negative for its two isoelectric points at pH 8.4 and 11.0,[32] which is favorable for the electrophilic addition of an amino group to site 2 but not for the Schiff base reaction. To optimize the yield, **6** was synthesized at a series of pH values from 6.0 to 14.0, from which the dependence of the yield on the pH was derived as shown in Figure S1 (in the Supporting Information). It was indicated that the yield was maximum (30%) at pH 9.5, 2 times more than what was ever reported, greatly promoting the pharmaceutical significance of the Schiff base derivatives.

Spectral Properties. Figure 1 shows the absorption spectra and fluorescence emission for **2** and **5**–**7** in dimethyl sulfoxide at the same concentration. Compared to **2**, a remarkable feature of the Schiff base derivatives is enhancement of the absorption of green (500–530 nm), orange (580 nm), and red (640 nm) light, and the emission peak shifts to 675 nm. The absorption of green or orange light matching a copper vapor laser (510, 580 nm) or Nd:YAG laser (532 nm) is favorable for PDT of microvascular diseases,[33−36] while the red absorption peak suggests that the derivatives are more favorable for PDT of tumors than their parent.[22,28,29]

dx.doi.org/10.1021/jm2017368 | J. Med. Chem. 2012, 55, 1910–1919

Solubility and Partition Coefficient. The solubility in phosphate-buffered saline (PBS) and partition coefficient (PC) were determined by the methods described in the Experimental Section. Table 1 lists the carbon atom number of the alkyl chain in the substituent, PC, and solubility for **5**−**7** along with those for **2**−**4** as references.

Table 1. Partition Coefficient (PC) and Solubility in PBS (*S*)

compd	carbon atom number	PC[a]	*S* in PBS[b] (mg/mL)
2	0	28.6 ± 0.6	(4.6 ± 0.4) × 10^{-3}
3	2	2.2 ± 0.4	9.2 ± 0.4
4	3	4.8 ± 0.3	6.6 ± 0.4
5	4	7.5 ± 0.5	3.9 ± 0.4
6	5	9.0 ± 0.4	1.7 ± 0.5
7	6	11.6 ± 0.4	0.2 ± 0.1

[a]PC is the mean partition coefficient ± SEM of three independent experiments. [b]*S* is the mean solubility ± SEM in PBS of three independent experiments.

Plots of the solubility and PC versus the carbon atom number are shown in Figure S2 in the Supporting Information. The linearity of the plots indicates that the quantitative solubility or optimized amphiphilicity can be determined as long as the clinically required concentration is known, which will be estimated in the last section.

Singlet Oxygen ($^1O_2$) Yields. Photosensitization activity is mainly evaluated by the singlet oxygen ($^1O_2$) yield for it is the most important species for the PDT effect.[2,37,38] Singlet oxygen yields were determined by the 9,10-diphenylanthracene (DPA) bleaching method for the derivatives with identical absorption under various light conditions. On the basis of the plots of decreases of DPA absorbance at 376 nm with irradiation time, the $^1O_2$ yield for **5**−**7** was estimated to be 0.94 ± 0.01, 0.98 ± 0.01, and 1.01 ± 0.01, respectively, with 0.76 for **2** as a reference,[39] and invariable under blue, orange, or red light or light of wavelengths larger than 470 nm (shown in Figure S3 in the Supporting Information), suggesting that a high $^1O_2$ yield is an intrinsic feature of the Schiff base derivatives.

Triplet-Excited-State Yields. Singlet oxygen may form via an energy transfer from a triplet excited photosensitizer to a ground-state oxygen molecule.[40,41] To search for the origin of the singlet oxygen, transient absorption spectra were selectively measured for structurally different **2**, **3**, and **6** after a pulse excitation, as shown parts A−C, respectively, in Figure 2. The positive peaks appearing at around 560 nm for **2** and **6** but 510 nm for **3** were ascribed to the triplet absorption, and plots of the peak amplitudes versus time are electively shown for the period of 0−1000 ns in Figure 2D. It can be seen that the maximum absorbance appears commonly at around 300 ns, ascribed to intersystem crossing. Figure 2E shows the decay trace of the peak absorbance for **2**, **3**, and **6**, from which the lifetime was estimated to be 9, 6, and 12 μs, respectively. By a comparative method[42] described on p S4 in the Supporting Information, the triplet-state yields for **3** and **6** were estimated to be 0.31 ± 0.01 and 1.00 ± 0.03, respectively, with 0.77 for **2** as a reference,[43] indicating that a high triplet-excited-state yield is a feature of the Schiff base derivatives.

Cellular and Liposome-Mimic Uptakes. Cellular uptake of **6** by human gastric carcinoma BGC823 cells was detected by a laser confocal fluorescence microscope, as shown in Figure 3. After the cells were incubated with **6** (1 μM) for 5 h, the red fluorescence image indicated uptake of **6**. However, the apparent fluorescence intensity is not necessarily equivalent to the amount of photosensitizer in various regions of the cell for it varies sensitively to the microenvironment polarity.[44−47]

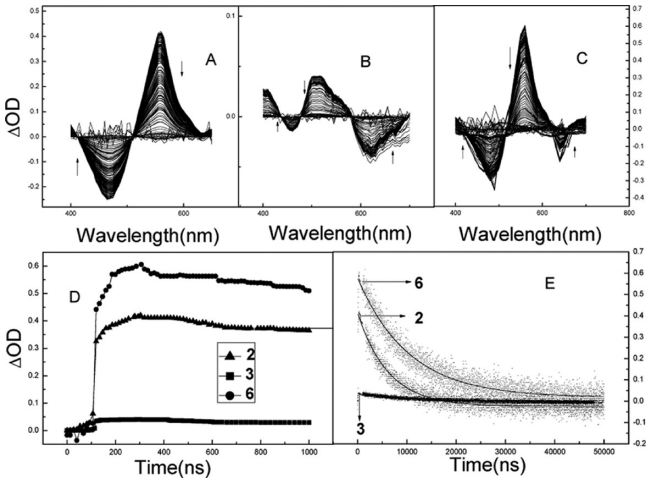

Figure 2. Transient absorption spectra recorded from 0 to 50 μs for **2** (A), **3** (B), and **6** (C) in deaerated cyclohexane. (D) Time-dependent absorbance at 560 nm for **2** and **6** and at 510 nm for **3** within 1 μs. (E) Transient decay trace of the absorbance at 560 nm for **2** and **6** and at 510 nm for **3**.

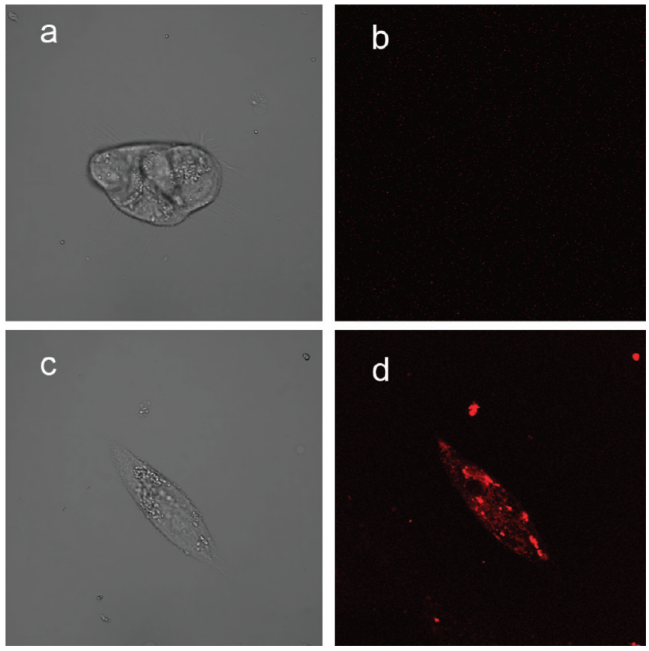

Figure 3. BGC823 cell images in bright field (a, c) and cellular fluorescence (b, d) in the absence and presence of **6**, respectively.

Alternatively, liposomes were used as a mimic biomembrane[48,49] to monitor the uptake quantity and kinetics. First, the absorption spectra in PBS were measured for **2**, **3**, and **6** in concentrations of 0.0−8.0 μM, which is less than the maximum solubility of **2** (8.8 μM[47]). Second, a plot of the absorbance versus concentration was derived as shown in Figure 4. Third, the slope value of each plot, reflecting the character of the derivative, was calculated and is listed in Table 2.

To monitor the molecular transportation of a derivative in PBS to liposomes, absorption spectra were measured at a series of times after **2**, **3**, or **6** in PBS (8 μM) was added to the liposome solution in PBS, from which a plot of the absorbance

dx.doi.org/10.1021/jm2017368 | J. Med. Chem. 2012, 55, 1910−1919

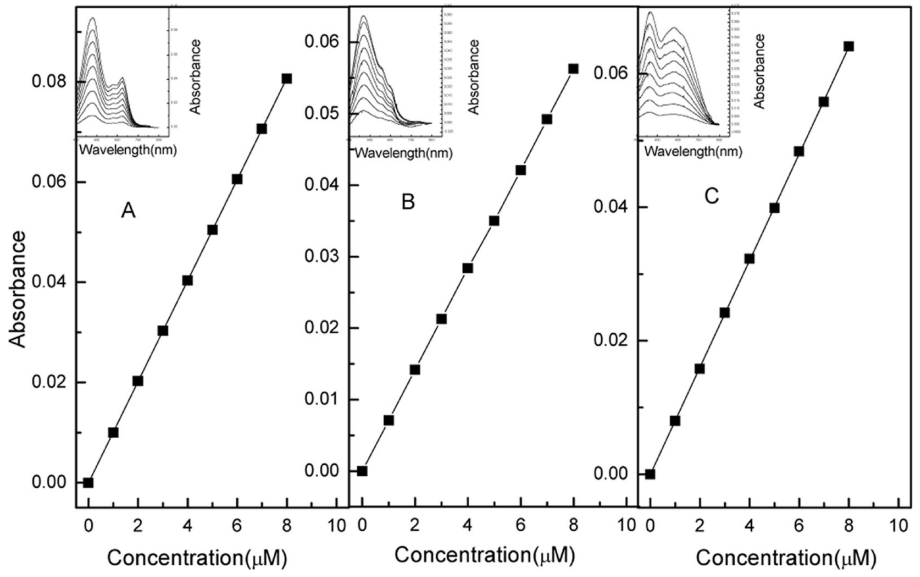

Figure 4. Maximum absorbance for **6** (A), **2** (B), and **3** (C) at a series of concentrations (from 0.0 to 8.0 μM) in PBS (pH 7.4). Insets: absorption spectra.

Table 2. Slopes of the Absorbance−Concentration Plots for 6, 2, and 3 in PBS (pH 7.4) and Those ahead of or behind the Intersections in Figure 6 as Well as the Correlative Coefficient (R)

compd	slope in PBS	R	slope ahead of the intersection	R	slope behind the intersection	R
2	0.0071	0.9999	0.0156	0.9999	0.0072	0.9999
3	0.0080	0.9999	0.0100	0.9998	0.0081	0.9998
6	0.0101	0.9999	0.0161	0.9999	0.0101	0.9999

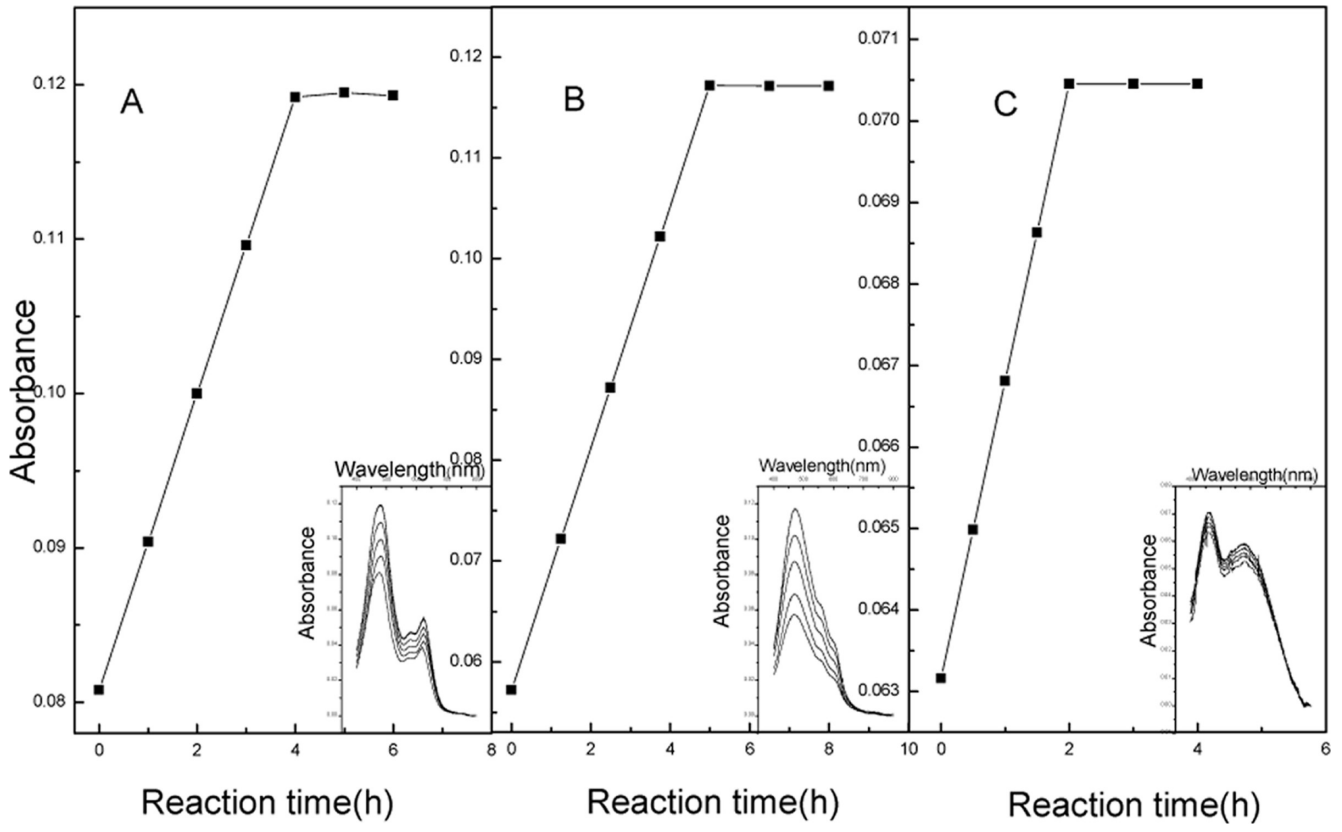

Figure 5. Time-dependent peak absorbance after addition of **6** (A), **2** (B), or **3** (C) (8 μM) in PBS to liposomes (0.08 g/L) in PBS (pH 7.4). Insets: absorption spectra measured at a series of times.

dx.doi.org/10.1021/jm2017368 | J. Med. Chem. 2012, 55, 1910−1919

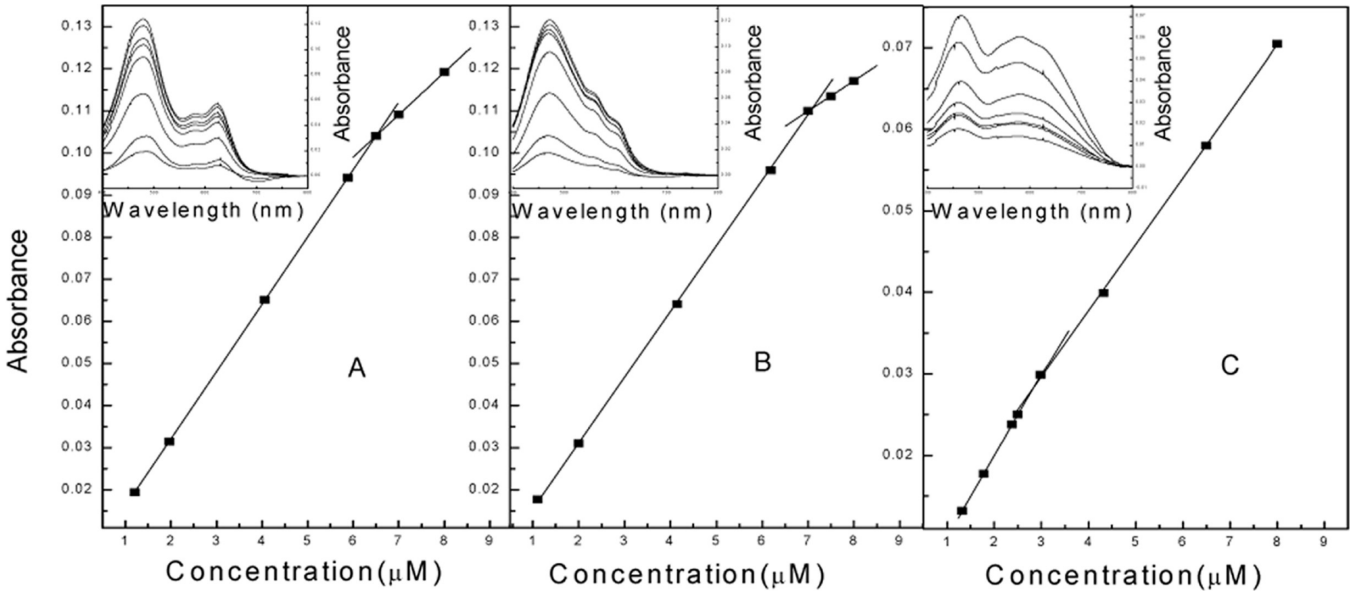

Figure 6. Maximum absorbance versus the concentration of **6** (A), **2** (B), and **3** (C) in PBS solution (pH 7.4) derived from absorption spectra (insets) measured 4, 5, and 2 h after addition to a PBS solution of liposomes.

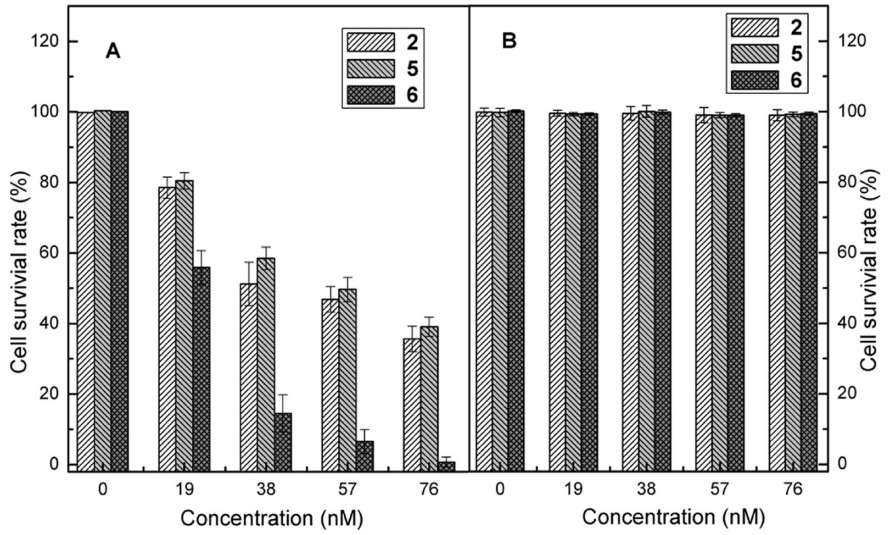

Figure 7. (A) Percent survival of human gastric cancer BGC823 cells in the presence of **2**, **5**, or **6** (0, 19, 38, 57, or 76 nM) and light (532 nm laser, 20 mW/cm^2, 1000 s). (B) Same as (A) but in the absence of light. Data were averaged from three independent experiments with the error range as indicated.

versus time was derived, as shown in Figure 5. The figure shows that the absorbance for **2**, **3**, and **6** increased linearly until 5, 2, and 4 h, respectively, suggesting the time at which the derivative reached equilibrium distribution between PBS and liposomes. It also indicates that a more hydrophilic derivative reaches equilibration faster. The saturation time is indicative of the cell incubation in the in vitro experiments.

To measure the maximum uptake for various derivatives, absorption spectra were measured after **2**, **3**, or **6** in a series of concentrations in PBS was added to liposomes at 5, 2, or 4 h, respectively, from which a plot of the absorbance versus concentration was derived, as shown in Figure 6. It can be seen that the plots for **2**, **3**, and **6** undergo a slope change at 7.0, 3.0, and 6.5 μM, respectively, and the slope values on both sides of the intersection point are listed in Table 2. The slope value behind the intersection point is exactly identical to that in PBS, while that ahead of the intersection point indicates the absorption feature in liposomes. This suggests that the maximum liposomal uptake of **2**, **3**, and **6** is 7.0, 3.0, and 6.5 μM in the experimental conditions. Reasonably, the uptake of **6** is nearly comparable to that of the parent **2**, while the most hydrophilic **3** exhibits the lowest uptake.

PDT Activity on Human Gastric Carcinoma BGC823 Cells. The human gastric carcinoma BGC823 cells were incubated for 5 h in the presence of **2**, **5**, or **6** (0−76 nM) followed by irradiation with a 532 nm laser of 20 J/cm^2 (20 mW/cm^2) for 1000 s or no irradiation. Parts A and B of Figure 7 show the estimated cell survivals with and without irradiation, respectively. It was confirmed that **2**, **5**, and **6** in the concentrations used had no dark toxicity to the cells and light did not result in any cell death independently, while the cell death was completely ascribed to the PDT effect. Estimated from the data in Figure 7A, IC_{50}, defined as the photosensitizer concentration required to kill 50% of the cells, is 40, 54, and 22

dx.doi.org/10.1021/jm2017368 | J. Med. Chem. 2012, 55, 1910−1919

Scheme 1. Procedure for the Synthesis of 4-Amino-1-butanesulfonic Acid (n = 4), 5-Amino-1-pentanesulfonic Acid (n = 5), and 6-Amino-1-hexanesulfonic Acid (n = 6)

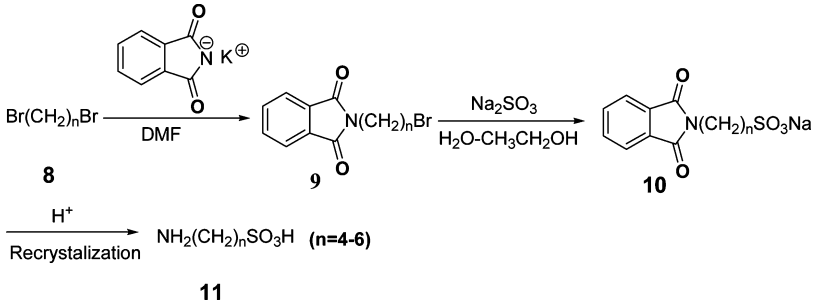

nM for **2**, **5**, and **6**, respectively. It can be seen from Figure 1 that the absorbances of **2** and **6** at 532 nm are almost identical; therefore, the higher PDT activity for **6** can be ascribed to photosensitization activity and cellular uptake. In fact, **6** is the first hypocrellin derivative to exhibit a higher PDT activity than its parent. At a certain concentration (76 nM) of **2**, **5**, and **6**, the cell survival is also a function of light dose, as shown in Figure S5 (in the Supporting Information), suggesting that light delivery is a key factor for the PDT activity.

On the basis of the relative PDT activity and **2** dosage in animal experiments as well as some clinical criteria, the clinically required concentration (C) was estimated to be around 0.8 mg/mL (p S2 in the Supporting Information). As listed in Table 1, the solubilities of **3**–**6** are all larger than the concentration; however, the largest PC for **6** predicts the largest cellular uptake. Consequently, it is concluded that **6** achieves optimized amphiphilicity. Interestingly, as shown in Figure S2 (Supporting Information), the linearly descending aqueous solubility or ascending PC illustrates a general significance for the optimized amphiphilicity or quantitative aqueous solubility.

It is a general rule that biological PDT activity in vitro correlates positively to that in vivo,[50−54] especially for microvascular diseases;[55,56] therefore, it is predictable that **6** is more PDT active in vivo than **2**. In vitro experiments should also have been done by the use of vasculature endothelial cells; however, it is expected that the result would be similar because the cellular structures are not so different from a photodynamic therapy point of view.[57,58] PDT could result in cell death via destruction of the membranes, cores, and organs or apoptosis;[59−61] however, the current work mainly concerns the photosensitizer efficiency to induce cell death but not the cell-death mechanism. Besides, red light is necessary for effective PDT of solid tumors but not of the cells. In fact, the much higher singlet oxygen yield for **6** under red light (in the Supporting Information) allows prediction of a higher cellular PDT activity than that of **2**; on the other hand, evaluating the PDT activity under red light is not equitable because the absorptions of **2** and **6** are incomparable.

CONCLUSIONS

Enlightened by quantitative aqueous solubility and the site-dependent photosensitization activity, three novel 17-substituted hypocrellin derivatives, **5**−**7**, were synthesized in a much higher yield than what was ever reported. **5**−**7** exhibit singlet oxygen yields of 0.94 ± 0.01, 0.98 ± 0.01, and 1.01 ± 0.01 and aqueous solubilities of 3.9, 1.7, and 0.2 mg/mL, respectively. **2**, **5**, and **6** exhibit IC_{50} values of 40, 22, and 54 nM, with no dark toxicity to human gastric carcinoma BGC823 cells. On the basis of the solubility, the relative PDT activity, and some clinical criteria, it can be concluded that **6** achieves quantitative solubility and optimized photosensitization activity at the same time and it is predicted that it can be directly deliverable without the need for any drug-delivery vehicles. The ideas presented in this work possess a common significance in medicinal chemistry.

EXPERIMENTAL SECTION

Materials. **1** was isolated from the fungus sacs of *Hypocrella bambusae* and recrystallized three times from acetone before use. **2** was prepared by dehydration of **1** in alkaline solution and purified by recrystallization twice from acetone.[62] Potassium phthalimide derivative was purchased from Acros Organics, and 1,4-dibromobutane, 1,5-dibromopentane, and 1,6-dibromohexane were purchased from Alfa Aesar. DPA was purchased from Aldrich Chemical Co. 1,4-Diazabicyclo[2.2.2]octane (DABCO) and dimethyl sulfoxide (DMSO) were purchased from Merck Co. Cyclohexane, dimethylformamide (DMF), deuterated solvents for ^{1}H NMR, and other agents of analytical grade were purchased from the Beijing Chemical Plant. PBS solution (pH 7.4) was composed of 1.4 mM KH_2PO_4, 6.4 mM Na_2HPO_4, 137 mM NaCl, and 2.6 mM KCl. Phosphate buffer, carbohydrate buffer, K_2CO_3−NaOH, and NaOH were used for pH ranges of 6.0−8.5, 8.5−10.5, 10.5−12.0, and >12.0, respectively. Water and DMF were redistilled, and the working solutions were prepared immediately before use.

Preparation of 5. 4-Amino-1-butanesulfonic acid (1200 mg, 7.84 mmol) and K_2CO_3 (1.7 g, 0.0123 mol) in 10 mL of water were mixed with **2** (100 mg, 0.189 mmol) in 10 mL of DMF and allowed to react at pH 9.5 under stirring and refluxing at 120 °C for 3 h in the dark. The solvent was removed under reduced-pressure evaporation. The residue was applied to a 1% citric acid−silica gel plate with dichloromethane/methanol (v/v = 5/1) used as the eluent. The gray-brown constituent was collected and further applied to a 1% citric acid−silica gel plate with ethyl acetate/methanol (v/v = 3/1) as the eluent, from which the gray-green component was collected and dried in vacuum to give a solid product (37 mg, 30%): UV−vis (DMSO, λ_{max}, log ε) 500 nm (4.31), 595 nm (3.90), 645 nm (4.13); IR (KBr, ν_{max}, cm^{-1}) 3443, 2940, 1711, 1616; ^{1}H NMR (400 MHz, MeOD-d_6, δ) 6.74, 6.52 (s, 2H, 5,8-H), 3.95−4.16 (m, 12H, 2,6,7,11-OCH_3), 3.66 (m, 2H, 19-CH_2), 3.52 (m, 2H, 22-CH_2), 3.14, 2.52 (d, 2H, 13-CH_2), 2.96 (s, 3H, 18-CH_3), 2.34 (s, 3H, 16-CH_3), 2.03−2.08 (m, 4H, 20,21-CH_2); ESI-MS (m/z) 662.3 (M − 1); HRMS (ESI, m/z) calcd for $C_{34}H_{34}O_{11}NS$ (M + H) 664.1847, found: 664.1847; HPLC (methol/water = 9/1) retention time 3.632 min. Anal. Calcd for $C_{34}H_{33}NO_{11}S$: C, 61.53; H, 5.01; N, 2.11; S, 4.83; Found: C, 61.38; H, 5.19; N, 2.04; S, 4.71.

Preparation of 6. Similar to the procedure described for **5**, a redistilled DMF solution (10 mL) of **2** (100 mg, 0.189 mmol) was mixed with a distilled water solution (10 mL) of 5-amino-1-pentanesulfonic acid (1000 mg, 5.98 mmol) and K_2CO_3 (1.5 g, 0.0109 mol) and allowed to react at pH 9.5. The product **6** was obtained as a gray-green solid (39 mg, 30%).: UV−vis (DMSO, λ_{max}, log ε) 499 nm (4.32), 593 nm (3.93), 640 nm (4.14); IR (KBr, ν_{max},

dx.doi.org/10.1021/jm2017368 | J. Med. Chem. 2012, 55, 1910−1919

cm^{-1}) 3494, 2939, 1699, 1610; ^1H NMR (400 MHz, MeOD-d_6, δ) 6.83, 6.77 (s, 2H, 5,8-H), 4.04−4.17 (m, 12H, 2,6,7,11-OCH_3), 3.65 (m, 2H, 19-CH_2), 3.49 (m, 2H, 23-CH_2), 3.14, 2.39 (d, 2H, 13-CH_2), 2.78 (s, 3H, 18-CH_3), 2.20 (s, 3H, 16-CH_3), 1.74−1.82 (m, 6H, 20,21,22-CH_2); ESI-MS (m/z) 676.3 (M − 1); HRMS (ESI, m/z) calcd for $C_{35}H_{36}O_{11}NS$ (M + H) 678.2004, found 678.2005; HPLC (methol/water = 9/1) retention time 3.687 min. Anal. Calcd for $C_{35}H_{35}NO_{11}S$: C, 62.03; H, 5.21; N, 2.07; S, 4.73 Found: C, 61.84; H, 5.48; N, 1.89; S, 4.63.

Preparation of 7. Similar to the procedures described for **5** and **6**, **2** (100 mg, 0.189 mmol) dissolved in 10 mL of redistilled DMF was mixed with 6-amino-1-hexanesulfonic acid (1200 mg, 6.63 mmol) and K_2CO_3 (1.5 g, 0.0109 mol) in 10 mL of distilled water and allowed to react at pH 9.5. **7** was obtained as a gray-green solid (39 mg, 30%): UV−vis (DMSO, λ_{max}, log ε) 498 nm (4.33), 593 nm (3.95), 642 nm (4.14); IR (KBr, ν_{max}, cm^{-1}) 3459, 2939, 1689, 1610; ^1H NMR (400 MHz, MeOD-d_6, δ) 6.75, 6.65 (s, 2H, 5,8-H), 3.93−4.18 (m, 12H, 2,6,7,11-OCH_3), 3.78 (m, 2H, 19-CH_2), 3.66 (m, 2H, 24-CH_2), 3.50, 2.06 (d, 2H, 13-CH_2), 2.87 (s, 3H, 18-CH_3), 2.37 (s, 3H, 16-CH_3), 1.65−1.77 (m, 8H, 20,21,22,23-CH_2); MALDI TOF MS (m/z) 690.4 (M − 1); HRMS (ESI, m/z) calcd for $C_{36}H_{38}O_{11}NS$ (M + H) 692.2160, found 692.2167; HPLC (methol/water = 9/1) retention time 4.008 min. Anal. Calcd for $C_{36}H_{37}NO_{11}S$: C, 62.51; H, 5.39; N, 2.02; S, 4.64; Found: C, 62.15; H, 5.63; N, 1.92; S, 4.50.

Preparation of Substituents. Because merchant 4-amino-1-butanesulfonic acid, 5-amino-1-pentanesulfonic acid, and 6-amino-1-hexanesulfonic acid are not available, the substituents were prepared according to Scheme 1. Generally, potassium phthalimide (32.30 mmol) and dibromoalkane (64.50 mmol) were mixed in DMF (75 mL) and allowed to react at room temperature for 18 h under stirring. KBr formed in the reaction was precipitated by adding acetone (75 mL) and removed by filtration, and then the solution was dried under reduced pressure. The residue was further purified by silica gel column chromatography (eluent hexanes/ethyl acetate = 10/1 (v/v)) to obtain a white solid, compound **9** (yield 72%). Compound **9** (23.15 mmol) and Na_2SO_3 (46.83 mmol) were dissolved in a mixed solvent of H_2O (140 mL)−95% ethyl acetate (85 mL) and allowed to react at 95 °C for 20 h with stirring. The reacted solution was dried under reduced pressure, and the residue was dissolved in water and washed three times with ethyl acetate. The aqueous layer was isolated and dried to obtain solid **10**. The solid was added to 37.5% HCl (73 mL) and allowed to react at 110 °C for 18 h with stirring. To get rid of the precipitates by filtration, the solution was washed three times with ethyl acetate. The aqueous layer was dried under reduced pressure to obtain a yellow solid which was further purified by recrystallization in water−95% ethanol to obtain the product (yield 50%). ^1H NMR for 4-amino-1-butanesulfonic acid (400 MHz, D_2O, δ): 3.50 (t, 2H), 2.68 (t, 2H), 1.50−1.65 (m, 4H). ^1H NMR for 5-amino-1-pentanesulfonic acid (400 MHz, D_2O, δ): 2.87 (t, 2H), 2.79 (t, 2H), 1.66−1.36 (m, 6H). ^1H NMR for 6-amino-1-hexanesulfonic acid (400 MHz, D_2O, δ): 2.93 (t, 2H), 2.86 (t, 2H), 1.35−1.75 (m, 8H).

Spectral Measurements. Steady-state absorption spectra were recorded on a Shimadzu UV-1601 spectrophotometer at room temperature. Infrared spectra were measured with a Bruker RF100/S spectrometer. Mass spectra were measured with a Fourier transform ion cyclotron resonance (FT-ICR) mass spectrometer, and proton nuclear magnetic resonance (^1H NMR) spectra were recorded with a Bruker Avance 400 spectrometer. The purities of the final compounds were determined using a Shimadzu LCsolution high-performance liquid chromatography (HPLC) system with a C-18 column (Shim-pack VP-ODS, 4.6 × 150 mm, 4.6 μm). High-resolution mass spectra were recorded with an APEXII FT-ICR mass spectrometer from Bruker Daltonics Inc. Elemental analyses were determined with a Flash EA 1112.

Partition Coefficients. Photosensitizers were dissolved in 1-octanol (2 mL) to a concentration of 20 μM, and then the same volume (2 mL) of PBS (pH 7.4) was added. The mixture was dispersed ultrasonically for 2 min and then centrifuged for 10 min to separate the two phases. The PC was determined by the ratio of photosensitizer concentration in 1-octanol to that in PBS solution via the Beer−Lambert law, PC = $(A_{octanol}\varepsilon_{PBS})/(\varepsilon_{octanol}A_{PBS})$. Here, $A_{octanol}$ and A_{PBS} are the maximum absorptions of photosensitizer in 1-octanol and PBS and $\varepsilon_{octanol}$ and ε_{PBS} are the molar extinction coefficients of photosensitizer in 1-octanol and PBS. $\varepsilon_{octanol}/\varepsilon_{PBS}$ for **5**−**7** was determined to be 1.95, 1.96, and 1.98, respectively, according to the Beer−Lambert law, that is, the absorbance in the same concentration in the two types of solvents.

Solubility in PBS Solution. **5**−**7** dissolved in PBS solution (pH 7.4) in a series of concentrations were stored in the dark for 12 h, and then the absorption spectra were measured, from which a plot of the absorbance versus the concentration for each photosenstizer was derived. The solubility was determined by the maximum value in the linear range of the plot.

Determination of the Singlet Oxygen Quantum Yield. The $^1O_2$ yields were determined by the DPA-bleaching method[39] under irradiation with a medium-pressure sodium lamp (450 W) with light of wavelengths longer than 470 nm, blue (400−480 nm), orange (580−600 nm), or red (600−700 nm) light. The photobleaching of DPA was monitored by the decrease in the absorbance at 376 nm. To make the results comparable, the concentrations of all of the photosensitizers were adjusted to give identical integrate area of the absorption.

Laser Flash Photolysis. Laser flash photolysis experiments were carried out on an Edinburgh LP920-laser flash photolysis spectrometer equipped with a Q-switched Nd:YAG laser to provide 532 nm light of 35 mJ and a 7 ns pulse. The analyzing beam source was generated by a pulsed xenon arc lamp (450 W, ozone free), and a photomultiplier tube was used as the detector. The kinetic curves of the transient absorption in the 400−700 nm range were recorded after the pulse excitation. Photosensitizer solution in cyclohexane was freshly prepared, and the concentration was adjusted to give the same optical density (0.58) at 532 nm. The solution was carefully deaerated by bubbling high-purity N_2 for at least 20 min before measurement at 20 °C under pure N_2.

Cellular Fluorescence Images. Exponentially grown human gastric carcinoma cells (BGC823 cells) in the culture medium (2 mL) were seeded on a coverslip at a density of 1×10^5 and incubated overnight at 37 °C under humidified air containing 5% CO_2. The medium was removed. Then the cells were incubated with **6** (1 μM) for 5 h at 37 °C containing 5% CO_2. The cells were rinsed three times with PBS and then observed with an Olympus FV1000 confocal microscope equipped with a 488 nm argon ion laser. Emission signals from 650 to 750 nm were collected. The control experiment was done under the same conditions but without photosensitizers.

Preparation of Photosensitizers in Liposomes. Liposomes were prepared by egg L-phosphatidylcholine (EPC) and cholesterol by using the film-ultrasonic technique.[63] **3** was prepared as described previously.[21] First, concentrated solutions of **2**, **3**, and **6** in DMSO (2 mg/mL) were slowly added to PBS (pH 7.4) to give a final concentration from 0 to 8 μM, and the absorbance spectra were measured. **2**, **3**, or **6** in each concentration in PBS was slowly added into the liposomal solution with stirring, and the absorption spectra were measured at a series of times.

Assessment of Cell Survival. The human gastric carcinoma cell line (BGC823 cells) used in this study was cultured in Dulbecco's modified Eagle's medium (DMEM) supplemented with 5% (v/v) fetal bovine serum (FBS), 1% (v/v) nonessential amino acids, penicillin (100 U/mL), and streptomycin (100 μg/mL) in 75 cm^2 flasks at 37 °C under humidified air containing 5% CO_2. The cells in logarithmic phase were detached by treatment with trypsin−ethylenediaminetetraacetic acid (EDTA)−PBS and diluted to a density of 5×10^5 cells/mL in the presence of DMEM supplemented with 5% FBS. The cell suspension was seeded in wells (100 μL each) in 96-well microplates and incubated under 5% CO_2 at 37 °C for 24 h. One column of wells did not receive cells to serve as the blank. Then the cells were changed to DMEM (FBS-free) medium containing photosensitizers in a series of concentrations (0, 19, 38, 57, and 76 nM) and incubated at 37 °C in the dark for 5 h. After removal of the above medium containing photosensitizers and addition of the fresh DMEM medium, the cells were irradiated with a 532 nm laser of 0−30 M_w/cm^2 for 1000 s and then incubated in the dark for 24 h before survival assessment.

Meanwhile, dark toxicity was measured under the same conditions without irradiation in parallel. The cell survival was estimated by the 3-(4,5-dimethylthiazol-2-yl)-2,5-diphenyltetrazolium bromide (MTT) assay.[64,65] Briefly, after 20 μL of MTT (5 mg/mL) was added to each well, the cells were further incubated for 90 min. MTT solution was removed, and 200 μL of DMSO was added to dissolve the formazan crystals. Then the plates were shaken at room temperature for 10 min, and the optical density at 570 nm was read on a microplate reader, from which cell survivals were derived.

■ ASSOCIATED CONTENT

Supporting Information

Dependence of the yields of **6** on the pH values, estimation of the clinically required concentration, linear plots of the PC or the solubility versus the carbon atom number in the substituent, dependence of the DPA absorbance decreases on the illumination time under various light conditions, estimation of the triplet-state yield Φ_T; light-dose-dependent cell survivals in the presence of a certain concentration (76 nM) of **2**, **5**, or **6**, ^{1}H NMR, MS, HRMS, and IR spectra of **5**−**7**, ^{1}H NMR spectra of 4-amino-1-butanesulfonic acid, 5-amino-1-pentanesulfonic acid, and 6-amino-1-hexanesulfonic acid, and HPLC analysis of **5**−**7**. This material is available free of charge via the Internet at http://pubs.acs.org.

■ AUTHOR INFORMATION

Corresponding Author

*Phone: +86-10-82617053 (J.Z.); +86-10-66939794 (Y.G.); +86-10-82617053 (J.X.). Fax: +86-10-82617315 (J.Z.); +86-10-68212522 (Y.G.); +86-10-82617315 (J.X.). E-mail: zhaojq@iccas.ac.cn (J.Z.); guyinglaser@sina.com (Y.G.); xiejie@iccas.ac.cn (J.X.).

Notes

The authors declare no competing financial interest.

■ ACKNOWLEDGMENTS

This project was supported by the National Natural Science Foundation of China (Grants 20872144 and 31170614).

■ ABBREVIATIONS USED

PDT, photodynamic therapy; HB, hypocrellin B; ROS, reactive oxygen species; AMD, age-related macular degeneration; PWS, port wine stain; $^1O_2$, singlet oxygen; PBS, phosphate-buffered saline; DPA, 9,10-diphenylanthracene; DABCO, 1,4-diazabicyclo[2.2.2]octane; DMSO, dimethyl sulfoxide; DMF, dimethylformamide; NMR, nuclear magnetic resonance; MS, mass spectrometry; HRMS, high-resolution mass spectrometry; HPLC, high-performance liquid chromatography; FBS, fetal bovine serum; EPC, egg L-phosphatidylcholine; DMEM, Dulbecco's modified Eagle's medium; EDTA, ethylenediaminetetraacetic acid; MTT, 3-(4,5-dimethylthiazol-2-yl)-2,5-diphenyltetrazolium bromide; PC, partition coefficient

■ REFERENCES

(1) Dolmans, D. E. J. G. J.; Fukumura, D.; Jain, R. K. Photodynamic therapy for cancer. *Nat. Rev. Cancer* **2003**, *3*, 380−387.

(2) Detty, M. R.; Gibson, S. L.; Wagner, S. J. Current clinical and preclinical photosensitizers for use in photodynamic therapy. *J. Med. Chem.* **2004**, *47*, 3897−3915.

(3) Brown, S. B.; Brown, E. A.; Walker, I. The present and future role of photodynamic therapy in cancer treatment. *Lancet Oncol.* **2004**, *5*, 497−508.

(4) Jori, G.; Fabris, C.; Soncin, M.; Ferro, S.; Coppellotti, O.; Dei, D.; Fantetti, L.; Chiti, G.; Roneucci, G. Photodynamic therapy in the treatment of microbial infections: Basic principles and perspective applications. *Lasers Surg. Med.* **2006**, *38*, 468−481.

(5) O'Brien, E. M.; Morgan, B. J.; Mulrooney, C. A.; Carroll, P. J.; Kozlowski, M. C. Perylenequinone natural products: Total synthesis of hypocrellin A. *J. Org. Chem.* **2010**, *75*, 57−68.

(6) Cai, Y. J.; Liang, X. H.; Liao, X. R.; Ding, Y. R.; Sun, J.; Li, X. H. High-yield hypocrellin A production in solid-state fermentation by *Shiraia* sp. SUPER-H168. *Appl. Biochem. Biotechnol.* **2010**, *160*, 2275−2286.

(7) Zhang, J.; Cao, E. H.; Li, J. F.; Zhang, T. C.; Ma, W. J. Photodynamic effects of hypocrellin A on three human malignant cell lines by inducing apoptotic cell death. *J. Photochem. Photobiol., B* **1998**, *43*, 106−111.

(8) Wang, Z. J.; He, Y. Y.; Huang, C. G.; Huang, J. S.; Huang, Y. C.; An, J. Y.; Gu, Y.; Jiang, L. J. Pharmacokinetics, tissue distribution and photodynamic therapy efficacy of liposomal-delivered hypocrellin A, a potential photosensitizer for tumor therapy. *Photochem. Photobiol.* **1999**, *70*, 773−780.

(9) An, H. B.; Xie, J.; Zhao, J. Q.; Li, Z. S. Photogeneration of free radicals ($^{\bullet}$OH and HB$^{\bullet}$) and singlet oxygen ($_1O_2$) by hypocrellin B in TX-100 micelles microsurroundings. *Free Radical Res.* **2003**, *37*, 1107−1112.

(10) Liu, Y. Y.; Wang, X. S.; Zhang, B. W. Hypocrellin-based photodynamic sensitizers. *Prog. Chem.* **2008**, *20*, 1345−1352.

(11) Beck, T. J.; Beyer, W.; Pongratz, T.; Stummer, W.; Waidelich, R.; Stepp, H.; Wagner, S.; Baumgartner, R. Clinical determination of tissue optical properties in vivo by spatially resolved reflectance measurements. *Photon Migr. Diffuse-Light Imaging* **2003**, *5138*, 96−105.

(12) Xu, S. J.; Zhang, X. X.; Chen, S.; Zhang, M. H.; Shen, T.; Wang, Z. P. Novel phototherapeutic agents: Investigation and progress of hypocrellin derivatives. *Chin. Sci. Bull.* **2003**, *48*, 1775−1785.

(13) Barsky, S. H.; Rosen, S.; Geer, D. E.; Noe, J. M. Nature and evolution of port wine stains—Computer-assisted study. *J. Invest. Dermatol.* **1980**, *74*, 154−157.

(14) Leung, C. K. S.; Chan, W. M.; Chong, K. K. L.; Chan, K. C.; Yung, W. H.; Tsang, M. K.; Tse, R. K. K.; Lam, D. S. C. Alignment artifacts in optical coherence tomography analyzed images. *Ophthalmology* **2007**, *114*, 263−270.

(15) Ishikawa, M.; Hashimoto, Y. Improvement in aqueous solubility in small molecule drug discovery programs by disruption of molecular planarity and symmetry. *J. Med. Chem.* **2011**, *54*, 1539−1554.

(16) Chowdhary, R. K.; Shariff, I.; Dolphin, D. Drug release characteristics of lipid based benzoporphyrin derivative. *J. Pharm. Pharm. Sci.* **2003**, *6*, 13−19.

(17) Xie, J.; Zhang, Y.; Zhao, J. Hypocrellin liposome formulation, comprises hypocrellin, phospholipids, cholesterol and lyophilization protecting agent. Patent CN101371828-A, Feb 25, 2009.

(18) Li, D. X.; Li, C. F.; Wang, A. H.; He, Q. A.; Li, J. B. Hierarchical gold/copolymer nanostructures as hydrophobic nanotanks for drug encapsulation. *J. Mater. Chem.* **2010**, *20*, 7782−7787.

(19) He, Y. Y.; Liu, H. Y.; An, J. Y.; Han, R.; Jiang, L. J. Photodynamic action of hypocrellin dyes: Structure-activity relationships. *Dyes Pigm.* **1999**, *44*, 63−67.

(20) Hu, Y. Z.; An, J. Y.; Jiang, L. J.; Chiang, L. C. Studies of the sulfonation of Hypocrellin-A and the photodynamic actions of the product. *J. Photochem. Photobiol., B* **1993**, *17*, 195−201.

(21) Zhao, Y. W.; Xie, J.; Ma, J. S.; Zhao, J. Q. A novel amphiphilic 2-taurine substituted hypocrellin B (THB) and its photodynamic activity. *New J. Chem.* **2004**, *28*, 484−489.

(22) Liu, X.; Xie, J.; Zhang, L. Y.; Chen, H. X.; Gu, Y.; Zhao, J. Q. A novel hypocrellin B derivative designed and synthesized by taking consideration to both drug delivery and biological photodynamic activity. *J. Photochem. Photobiol., B* **2009**, *94*, 171−178.

(23) He, H.; Lo, P. C.; Yeung, S. L.; Fong, W. P.; Ng, D. K. P. Synthesis and in vitro photodynamic activities of pegylated distyryl boron dipyrromethene derivatives. *J. Med. Chem.* **2011**, *54*, 3097−3102.

(24) He, Y. Y.; An, J. Y.; Zou, W.; Jiang, L. J. Photoreactions of hypocrellin B with thiol compounds. *J. Photochem. Photobiol., B* **1998**, *44*, 45−52.
(25) Xia, S. Q.; Zhou, J. H.; Chen, J. R.; Wang, X. S.; Zhang, B. W. A tyrosine-modified hypocrellin B with affinity for and photodamaging ability towards calf thymus DNA. *Chem. Commun.* **2003**, 2900−2901.
(26) Liu, Y. Y.; Zhou, Q. X.; Zeng, Z. H.; Qiao, R.; Wang, X. S.; Zhang, B. W. Photodynamic properties of a bispyrrolecarboxamide-modified hypocrellin B: The role of affinity and ascorbic acid. *J. Phys. Chem. B* **2008**, *112*, 9959−9965.
(27) Liu, X.; Xie, J.; Zhang, L. Y.; Chen, H. X.; Gu, Y.; Zhao, J. Q. Optimization of hypocrellin B derivative amphiphilicity and biological activity. *Chin. Sci. Bull.* **2009**, *54*, 2045−2050.
(28) Li, L.; Chen, Y. W.; Shen, J. Q.; Zhang, M. H.; Shen, T. New long-wavelength perylenequinones: Synthesis and phototoxicity of hypocrellin B derivatives. *Biochim. Biophys. Acta, Gen. Subj.* **2000**, *1523*, 6−12.
(29) Zhao, Y. W.; Zhao, J. Q. Preparation of a novel hypocrellin derivative and its photochemical, photophysical properties. *Dyes Pigm.* **2004**, *63*, 175−179.
(30) Electrolytes, electromotive force, and chemical equilibrium. In *Lange's Handbook of Chemistry*, 15th ed.; Dean, J. A., Ed.; McGraw-Hill: Knoxville, TN, 1999; pp 8.26−8.26.
(31) Tang, Y. J.; Liu, H. Y.; An, J. Y.; Han, R. Synthesis, characterization and photodynamic activity of amino-substituted hypocrellin derivatives. *Photochem. Photobiol.* **2001**, *74*, 201−205.
(32) He, Y. Y.; An, J. Y.; Jiang, L. J. pH Effect on the spectroscopic behavior and photoinduced generation of semiquinone anion radical of hypocrellin B. *Dyes Pigm.* **1999**, *41*, 79−87.
(33) Zhao, J. Q.; Deng, H.; Xie, J.; Liu, X.; Zhang, Y.; Huang, N. Y.; Gu, Y. Towards characteristics of photodynamic drugs specifically aimed at microvascular diseases. *Mini-Rev. Med. Chem.* **2010**, *10*, 332−341.
(34) Liu, H. L. L., F.G.; Gu, Y.; Ma, J. H.; Zhao, J. Q.; Zeng, J.; Li, X. S. An experimental study of photodynamic effect of hypocrelline B liposome on leghorn cock comb. *Chin. J. Laser Med. Surg.* **2005**, *14*, 1−5.
(35) Van, G. M. J.; Welch, A. J.; Pickering, J. W.; Tan, O. T.; Gijsbers, G. H. Wavelengths for laser treatment of port wine stains and telangiectasia. *Lasers Surg. Med.* **1995**, *16*, 147−155.
(36) Mimoun, G.; Cochard, C.; Ouali, K.; Zourdani, A.; Soubrane, G.; Coscas, G. Evaluation of frequency-doubled Nd-Yag versus krypton red laser for photocoagulation of extra foveal and juxta foveal choroidal neovascularization due to age-related maculopathy (A.M.D.). *Vision Res.* **1995**, *35*, 4125−4125.
(37) Grossweiner, L. I. In *The Science of Phototherapy: An Introduction*; John, L. R., Ed.; Springer: Dordrecht, The Netherlands, 2005; pp 1−8.
(38) Obata, M.; Hirohara, S.; Tanaka, R.; Kinoshita, I.; Ohkubo, K.; Fukuzumi, S.; Tanihara, M.; Yano, S. In vitro heavy-atom effect of palladium(II) and platinum(II) complexes of pyrrolidine-fused chlorin in photodynamic therapy. *J. Med. Chem.* **2009**, *52*, 2747−2753.
(39) Diwu, Z. J.; Lown, J. W. Photosensitization by anticancer agents 0.12. Perylene quinonoid pigments, a novel type of singlet oxygen sensitizer. *J. Photochem. Photobiol., A* **1992**, *64*, 273−287.
(40) Pandey, R. K.; Constantine, S.; Tsuchida, T.; Zheng, G.; Medforth, C. J.; Aoudia, M.; Kozyrev, A. N.; Rodgers, M. A. J.; Kato, H.; Smith, K. M.; Dougherty, T. J. Synthesis, photophysical properties, in vivo photosensitizing efficacy, and human serum albumin binding properties of some novel bacteriochlorins. *J. Med. Chem.* **1997**, *40*, 2770−2779.
(41) Dumas, S.; Lepretre, J. C.; Lepellec, A.; Darmanyan, A.; Jardon, P. Reactivity of the photo excited forms of hypericin, hypocrellin A, hypocrellin B and methylated hypericin towards molecular oxygen the role of charge transfer interaction. *J. Photochem. Photobiol., A* **2004**, *163*, 297−306.
(42) Nyokong, T.; Idowu, M. Synthesis, photophysics and photochemistry of tin(IV) phthalocyanine derivatives. *J. Photochem. Photobiol., A* **2008**, *199*, 282−290.
(43) Jiang, L. J.; He, Y. Y. Photophysics, photochemistry and photobiology of hypocrellin photosensitizers. *Chin. Sci. Bull.* **2001**, *46*, 6−16.
(44) Zhao, B. Z.; Xie, H.; Zhao, J. Q. Binding of hypocrellin B to human serum albumin and photo-induced interactions. *Biochim. Biophys. Acta, Gen. Subj.* **2005**, *1722*, 124−130.
(45) Zhao, B. Z.; Song, L. M.; Liu, X.; Xie, H.; Zhao, J. Q. Spectroscopic studies of the interaction between hypocrellin B and human serum albumin. *Bioorg. Med. Chem.* **2006**, *14*, 2428−2432.
(46) Song, L. M.; Zhao, B. Z.; Xie, H.; Zhao, J. Q. Interactions of hypocrellin B with hyaluronan and photo-induced interactions. *Biochim. Biophys. Acta, Gen. Subj.* **2006**, *1760*, 333−339.
(47) Song, L. M.; Xie, J.; Zhang, C. X.; Li, C.; Zhao, J. Q. Recognition of various biomolecules by the environment-sensitive spectral responses of hypocrellin B. *Photochem. Photobiol. Sci.* **2007**, *6*, 683−688.
(48) Saija, A.; Scalese, M.; Lanza, M.; Marzullo, D.; Bonina, F.; Castelli, F. Flavonoids as antioxidant agents—Importance of their interaction with biomembranes. *Free Radical Biol. Med.* **1995**, *19*, 481−486.
(49) Fahr, A.; van Hoogevest, P.; May, S.; Bergstrand, N.; Leigh, M. L. S. Transfer of lipophilic drugs between liposomal membranes and biological interfaces: Consequences for drug delivery. *Eur. J. Pharm. Sci.* **2005**, *26*, 251−265.
(50) Lim, D. S.; Ko, S. H.; Won, D. H.; Lee, C. H.; Lee, W. Y. Photodynamic anti-tumor activity of a new chlorin-based photosensitizer against Lewis lung carcinoma cells in vitro and in vivo. *J. Porphyrins Phthalocyanines* **2003**, *7*, 155−161.
(51) Kirveliene, V.; Grazeliene, G.; Dabkeviciene, D.; Micke, I.; Kirvelis, D.; Juodka, B.; Didziapetriene, J. Schedule-dependent interaction between Doxorubicin and mTHPC-mediated photodynamic therapy in murine hepatoma in vitro and in vivo. *Cancer Chemother. Pharmacol.* **2006**, *57*, 65−72.
(52) Kralova, J.; Briza, T.; Moserova, I.; Dolensky, B.; Vasek, P.; Pouckova, P.; Kejik, Z.; Kaplanek, R.; Martasek, P.; Dvorak, M.; Kral, V. Glycol porphyrin derivatives as potent photodynamic inducers of apoptosis in tumor cells. *J. Med. Chem.* **2008**, *51*, 5964−5973.
(53) Sehgal, I.; Sibrian-Vazquez, M.; Vicente, M. G. H. Photoinduced cytotoxicity and biodistribution of prostate cancer cell-targeted porphyrins. *J. Med. Chem.* **2008**, *51*, 6014−6020.
(54) Lim, S. H.; Thivierge, C.; Nowak-Sliwinska, P.; Han, J. Y.; van den Bergh, H.; Wagnieres, G.; Burgess, K.; Lee, H. B. In vitro and in vivo photocytotoxicity of boron dipyrromethene derivatives for photodynamic therapy. *J. Med. Chem.* **2010**, *53*, 2865−2874.
(55) Strauss, W. S. L.; Sailer, R.; Schneckenburger, H.; Akgun, N.; Gottfried, V.; Chetwer, L.; Kimel, S. Photodynamic efficacy of naturally occurring porphyrins in endothelial cells in vitro and microvasculature in vivo. *J. Photochem. Photobiol., B* **1997**, *39*, 176−184.
(56) Okunaka, T.; Usuda, J.; Ichinose, S.; Hirata, H.; Ohtani, K.; Maehara, S.; Inoue, T.; Imai, K.; Kubota, M.; Tsunoda, Y.; Kuroiwa, Y.; Tsutsui, H.; Furukawa, K.; Nishio, K.; Kato, H. A possible relationship between the anti-cancer potency of photodynamic therapy using the novel photosensitizer ATX-s10-Na(II) and expression of the vascular endothelial growth factor in vivo. *Oncol. Rep.* **2007**, *18*, 679−683.
(57) Ball, D. J.; Mayhew, S.; Vernon, D. I.; Griffin, M.; Brown, S. B. Decreased efficiency of trypsinization of cells following photodynamic therapy: Evaluation of a role for tissue transglutaminase. *Photochem. Photobiol.* **2001**, *73*, 47−53.
(58) Reya, T.; Morrison, S. J.; Clarke, M. F.; Weissman, I. L. Stem cells, cancer, and cancer stem cells. *Nature* **2001**, *414*, 105−111.
(59) Ochsner, M. Photophysical and photobiological processes in the photodynamic therapy of tumours. *J. Photochem. Photobiol., B* **1997**, *39*, 1−18.
(60) Oleinick, N. L.; Morris, R. L.; Belichenko, T. The role of apoptosis in response to photodynamic therapy: What, where, why, and how. *Photochem. Photobiol. Sci.* **2002**, *1*, 1−21.
(61) Castano, A. P.; Mroz, P.; Hamblin, M. R. Photodynamic therapy and anti-tumour immunity. *Nat. Rev. Cancer* **2006**, *6*, 535−545.

(62) Zhao, K. H.; Jiang, L. J. Conversion of hypocrellin A in alkaline and neutral media. *Chin. J. Org. Chem.* **1989**, *9*, 252−254.
(63) Szoka, F.; Papahadjopoulos, D. Comparative properties and methods of preparation of lipid vesicles (liposomes). *Annu. Rev. Biophys. Biol.* **1980**, *9*, 467−508.
(64) Vellonen, K. S.; Honkakoski, P.; Urtti, A. Substrates and inhibitors of efflux proteins interfere with the MTT assay in cells and may lead to underestimation of drug toxicity. *Eur. J. Pharm. Sci.* **2004**, *23*, 181−188.
(65) Stefflova, K.; Chen, J.; Marotta, D.; Li, H.; Zheng, G. Photodynamic therapy agent with a built-in apoptosis sensor for evaluating its own therapeutic outcome in situ. *J. Med. Chem.* **2006**, *49*, 3850−3856.